EuroSun2026

INTERANNUAL SPATIAL AND TEMPORAL SOLAR IRRADIANCE VARIABILITY IN CANADA (1998-2022)

Bryanna Warriner[1,2], Erin Tonita[1], Lucio Mesquita[1]

1. CanmetENERGY-Ottawa, Natural Resources Canada, Ottawa, ON, Canada
2. University of Waterloo, Waterloo, ON, Canada

Corresponding author email: erin.tonita@nrcan-rncan.gc.ca

Summary

This study assesses annual and monthly solar irradiance variability across Canada over a 25-year period (1998-2022) using ERA5 reanalysis data on a 31×31 km grid, with spatial irradiance maps based on a reference year of 2025. Global horizontal irradiance (GHI) and beam horizontal irradiance (BHI) are analyzed using the coefficient of variation to compare annual and monthly variability. The 2025 spatial analysis shows a clear latitudinal gradient, with the highest solar resource concentrated in the southern interior of Canada, including the Prairie provinces and southern Ontario. The variability assessment indicates that GHI is relatively stable across most of Canada from year-to-year, while BHI is more sensitive to interannual atmospheric variation, especially at higher latitudes and coastal regions. Comparison with a higher-accuracy satellite-derived irradiance dataset, CWEEDS, confirms broad GHI variability patterns at select Canadian locations, with larger differences observed in some northern and coastal cities, indicating that data product selection can influence variability estimates.

Keywords: Solar resource, solar energy, irradiance, variability, Canada, interannual analysis, reanalysis, satellite

Field of application for the findings: Solar Resources and Energy Meteorology

Addressed audience: Solar resource researchers; users of solar data (industry, government, and academic).

1. Introduction

Understanding spatial and temporal trends of solar irradiance and its variability is essential to the application and development of solar energy, particularly as the installed global capacity of solar photovoltaics (PV) continues to grow (Lohmann *et al*. 2016). Quantifying irradiance variability improves the reliability and predictability of solar energy assessments, supporting PV system planning, financing, electrical grid stability, storage technology sizing, and dispatch strategies (Gerald *et al*. 2016). The variability of solar irradiance is driven by many influencing factors, including meteorological conditions, natural disturbances, and solar cycles, and varies depending on geographical location and climate patterns (Habte, A. *et al*., 2020). Irradiance variability can be quantified from a minutely timescale to a solar-cycle scale, supporting applications from grid-dynamics analysis to global climate change monitoring (Solanki, S. *et al*., 2013).

Although national and continental-scale assessments of solar variability have been conducted in regions such as Australia (Davy, R, & Troccoli, A., 2012), comparatively little research has focused on solar resource variability in polar and high-latitude regions. In a 2020 study by the National Renewable Energy Laboratory (NREL), Habte *et al*. characterized global horizontal irradiance (GHI) and direct normal irradiance (DNI) variability in the National Solar Radiation Database (NSRDB) across North America from 1998-2017 (Habte, A. *et al*., 2020). The geographical coverage of this dataset was limited to below 58°N at the time of publication and therefore did not represent Canada's full geospatial extent. This limitation highlights the need for a comprehensive assessment of solar irradiance across Canada, with particular emphasis on Arctic territories where knowledge of irradiance variability is crucial for increasing renewable energy penetration in remote microgrid communities. In this work, we examine interannual trends and seasonal variability of solar irradiance across Canada for 1998 to 2022. Our analysis highlights regional and climate-driven differences in irradiance variability, as well as differences between reanalysis and satellite-derived datasets.

2. Methods

2.1. Irradiance Data

Irradiance variability was examined using two different weather datasets: (1) the fifth-generation atmospheric reanalysis dataset (ERA5) produced by the European Centre for Medium-Range Weather Forecasts (ECMWF) (Hersbach *et al*. 2023), and (2) the Canadian Weather Energy and Engineering Datasets (CWEEDS), which underlying SolarAnywhere satellite model provides irradiance data at CWEEDS locations (NRCan, 2022). The ERA5 and CWEEDS irradiance datasets are among the most accurate solar irradiance datasets for reanalysis and satellite models in Canada, respectively (Tonita *et al.* 2026). Table 1 summarizes the key features of these two datasets.

Table 1: Summary of irradiance models used in this study.

Dataset Name	Organization	Model Type	Coverage	Irradiance Variables	Spatial Resolution	Data Range
ERA5	ECMWF	Reanalysis	Global	GHI, BHI	0.25° x 0.25° (31 km)	1940-present
CWEEDS	NRCan	Satellite-derived	Canada	GHI, DNI, DHI	649 sites	1998-2022

All spatial analyses were conducted using the Canada Albers Equal Area Conic projection to ensure accurate representation across Canada's geospatial domain. As the CWEEDS dataset contains information for 649 discrete locations in Canada rather than a continuous grid, the primary cross-Canada analysis was carried out using ERA5 for GHI and beam horizontal irradiance (BHI), the horizontal component of DNI. Although satellite-derived products often outperform reanalysis products for irradiance variables (Yang and Bright, 2020), ERA5 is used here as the primary dataset due to its accessibility.

Irradiance variability was calculated for GHI and BHI variables by converting hourly irradiance data to mean daily total irradiance (kWh/m^2/day) under different temporal scales (annually and monthly). An assessment period of 25 years (1998-2022 inclusive) was used to evaluate long-term and seasonal trends in irradiance patterns throughout Canada.

2.2. Calculation of Interannual Irradiance Variability

Solar irradiance variability was calculated using the coefficient of variation (COV). COV quantifies the temporal variability of solar irradiance relative to the mean solar irradiance for a given location, allowing for variability to be compared consistently across regions with different absolute annual irradiance. The COV is defined as:

$$COV = \frac{\sigma}{\mu} \times 100\% \qquad \text{(eq. 1)}$$

Where $\boldsymbol{\sigma}$ is the standard deviation and $\boldsymbol{\mu}$ represents the long-term mean of the dataset across the timeseries. For each ERA5 grid cell, annual mean daily total irradiance was calculated for GHI and BHI for each year in the 25-year period. The interannual COV was then calculated from the 25 annual values. The COV was similarly computed by grouping values by calendar month across the 25-year period, allowing seasonal variability to be assessed independently from annual variability.

3. Results

3.1. Spatial Distribution of Irradiance for 2025

As a reference for interannual variability results, the spatial patterns of mean daily total irradiance were examined for 2025 using gridded ERA5 data. Average GHI across Canada is given in Figure 1 and average BHI is given in Figure 2. Both irradiance maps exhibit a clear south-to-north gradient. The highest irradiance values occur primarily in the southern interior, including the prairie provinces and southern Ontario. In 2025, southern Alberta and Saskatchewan had the highest values in both datasets, with GHI exceeding 4 kWh/m^2/day and BHI exceeding 3 kWh/m^2/day in the highest-resource areas.

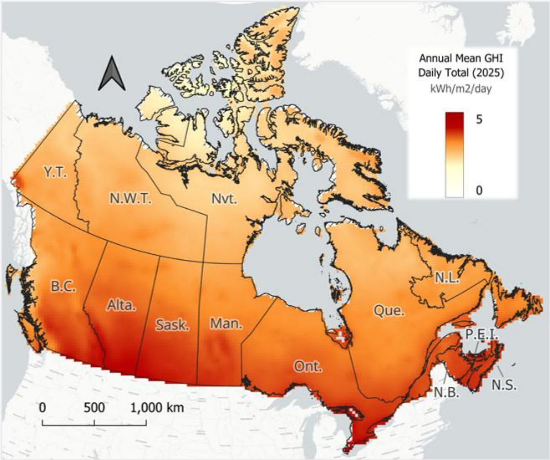

Figure 1: The annual mean daily GHI in 2025.

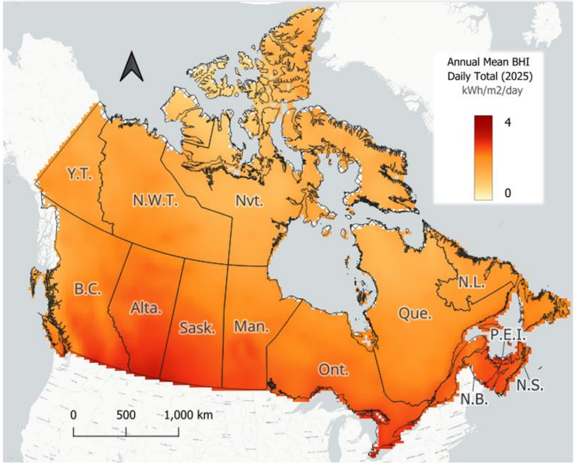

Figure 2: The annual mean daily BHI in 2025.

These spatial patterns also show that some high-latitude regions in Canada receive annual irradiance totals comparable to established PV markets in northern and central Europe. For example, Yellowknife at 62.4°N had an annual mean daily GHI of 3.02 kWh/m^2/day for 2025, while Berlin, Germany, at 52.5°N had an annual mean daily GHI of 3.06 kWh/m^2/day. Some high-latitude regions in Canada retain meaningful annual solar resource potential despite strong seasonality, reinforcing the importance of evaluating both annual totals and seasonal variability for northern PV applications.

Table 2 summarizes the 2025 mean daily total GHI and BHI for select cities in Canada. Toronto, Charlottetown, and Regina had the highest capital-city average GHI values, with around 3.9 kWh/m^2/day. The territorial capitals had lower annual mean GHI than capitals south of 60°N; Whitehorse, Yellowknife, and Iqaluit received approximately 2.6-3.0 kWh/m^2/day. BHI showed a similar pattern, with the lowest value in Iqaluit, reflecting the combined influence of high-latitude, seasonal daylight availability, and atmospheric conditions on the direct irradiance component.

Table 2: Mean daily total irradiance for capital cities in Canada from ERA5.

Capital City	Latitude (°N)	Longitude (°W)	GHI (kWh/m^2/day)	BHI (kWh/m^2/day)
Toronto, ON	43.6	79.3	3.95	2.59
Halifax, NS	44.6	63.5	3.73	2.52
Ottawa, ON	45.4	75.6	3.73	2.44
Fredericton, NB	45.9	66.6	3.71	2.37
Charlottetown, PE	46.2	63.1	3.93	2.57
Quebec City, QC	46.8	71.2	3.64	2.34
St. John's, NL	47.5	52.7	3.43	2.07
Victoria, BC	48.4	123.3	3.72	2.38
Winnipeg, MB	49.8	97.1	3.76	2.53
Regina, SK	50.4	104.6	3.86	2.56
Edmonton, AB	53.5	113.5	3.78	2.55
Whitehorse, YK	60.7	135	2.94	1.76
Yellowknife, NT	62.4	114.3	3.02	1.92
Iqaluit, NU	63.7	68.5	2.56	1.26

3.2. Interannual Irradiance Variability

Figure 3 and Figure 4 show the interannual COV for GHI and BHI using the ERA5 reanalysis dataset. Interannual variability shows clear regional structure, with higher values in northern Canada and many coastal regions compared with the southern interior. GHI variability is relatively low at a national scale compared to BHI variability, generally remaining below 5% COV, indicating that annual GHI is comparably stable from year-to-year. As a contrast, BHI variability is much higher, reaching ~20% in the highest-variability regions. This difference reflects the stronger sensitivity of the direct irradiance component to year-to-year changes in cloud cover, aerosols, water vapour, and other atmospheric conditions.

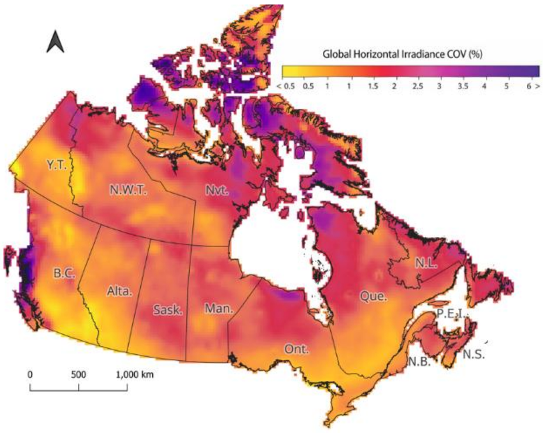

Figure 3. ERA5 interannual GHI COV from 1998-2022.

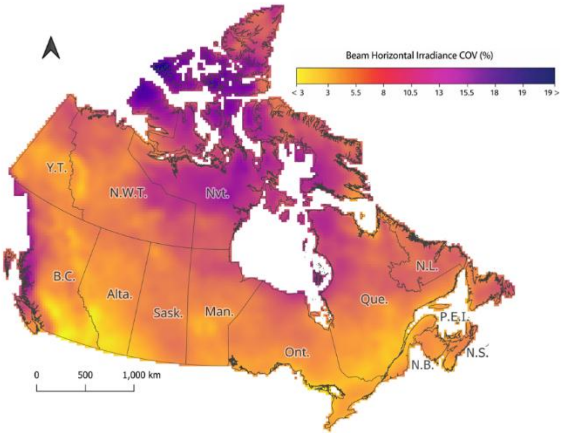

Figure 4. ERA5 interannual BHI COV from 1998-2022.

3.3. Interannual Monthly Irradiance Variability

Monthly interannual variability was assessed to determine whether annual COV masks important seasonal differences in solar resource stability. Figures 5 and 6 show monthly COV for GHI and BHI, respectively, calculated across the 1998-2022 period. Grey regions indicate areas where the monthly daily average irradiance falls below 0.05 kWh/m^2/day, as in the case above the Arctic circle around winter solstice. The monthly results show that variability is not uniform throughout the year and that seasonal patterns differ between GHI and BHI.

For GHI, the highest monthly interannual variability occurs primarily during the late spring and summer, with elevated COV values across much of Canada from May through September. During this period, variability is especially pronounced in northern and eastern regions around Hudson Bay. In contrast, the western coastal region shows its highest variability during winter months. Winter GHI COV is lower across much of the mapped ERA5 domain, which differs from the seasonal pattern reported by Habte *et al*. (2020) using NSRDB satellite irradiance data for southern Canada. Habte *et al.*, found significantly higher GHI COV from November through February for most Canadian regions below 58°N during 1998-2017. This discrepancy may reflect differences between reanalysis and satellite-derived datasets, as well as the challenges of interpreting winter variability in northern climates where irradiance values and daylight availability are low.

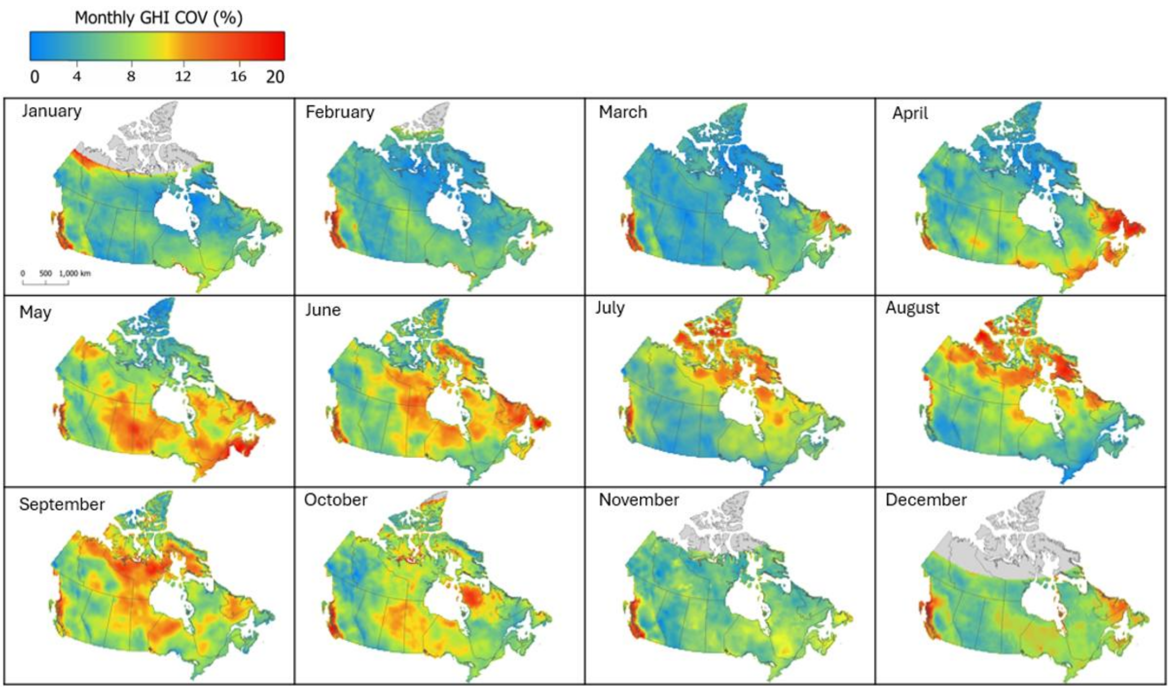

Figure 5. Monthly irradiance COV for GHI from 1998-2022 across Canada using ERA5.

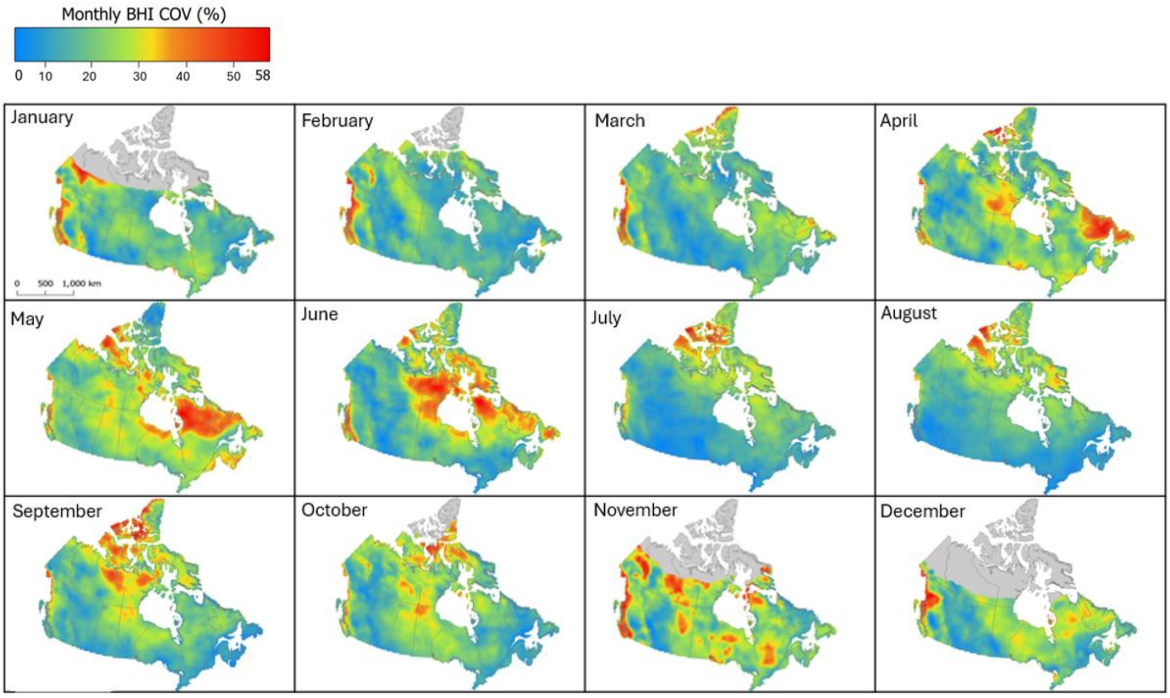

Figure 6. Monthly irradiance COV for BHI from 1998-2022 across Canada using ERA5.

For BHI, monthly interannual variability is substantially higher than for GHI across most months and regions. Elevated BHI COV occurs across northern Canada and around Hudson Bay during late spring, and summer, with additional winter variability along parts of the western coast. The monthly BHI results indicate that the direct irradiance component is less stable than global irradiance at both annual and seasonal timescales, which has implications for technologies and performance models that primarily depend on the direct beam component, such as solar tracking technologies.

3.4. CWEEDS Irradiance Variability

The ERA5 results were compared with CWEEDS to evaluate whether a higher-accuracy satellite-derived dataset produces similar interannual GHI variability patterns at point locations. As CWEEDS is available for discrete stations, rather than a continuous national grid, the comparison was performed for provincial, territorial, and federal capital cities. Table 3 compares 2025 mean daily irradiance values from ERA5 with interannual COV values from ERA5 and CWEEDS for the 1998-2022 assessment period. Since CWEEDS provides DNI data in place of BHI, the comparison can only be done over GHI.

Table 3. Comparison of interannual variability between data sources for capital cities in Canada.

Capital City	Latitude (°N)	Longitude (°W)	GHI ($kWh/m^2/day$)	BHI ($kWh/m^2/day$)	BHI COV (%)	GHI COV (%)	GHI COV (%)
			ERA5				CWEEDS
Toronto, ON	43.6	79.3	3.95	2.59	5.01	2.78	3.08
Halifax, NS	44.6	63.5	3.73	2.52	6.01	3.25	3.47
Ottawa, ON	45.4	75.6	3.73	2.44	4.64	2.51	2.66
Fredericton, NB	45.9	66.6	3.71	2.37	5.12	3.18	3.06
Charlottetown, PE	46.2	63.1	3.93	2.57	5.41	2.71	3.98
Quebec City, QC	46.8	71.2	3.64	2.34	4.40	2.47	2.79
St. John's, NL	47.5	52.7	3.43	2.07	7.62	3.92	4.38
Victoria, BC	48.4	123.3	3.72	2.38	5.13	2.71	3.83
Winnipeg, MB	49.8	97.1	3.76	2.53	5.52	2.96	2.73
Regina, SK	50.4	104.6	3.86	2.56	6.40	3.30	3.71
Edmonton, AB	53.5	113.5	3.78	2.55	4.39	2.47	2.55
Whitehorse, YK	60.7	135	2.94	1.76	6.48	2.96	2.36
Yellowknife, NT	62.4	114.3	3.02	1.92	6.48	3.02	2.08
Iqaluit, NU	63.7	68.5	2.56	1.26	7.88	3.89	5.01

CWEEDS and ERA5 show broadly consistent GHI variability patterns across capital cities, with GHI COV values differing by less than 0.5% abs. in most locations. The largest discrepancies (>0.5% abs. COV) occur in select northern and coastal locations of Charlottetown, Victoria, Yellowknife, and Iqaluit. Additionally, ERA5 tends to under-estimate variability compared to CWEEDS, although this pattern is not uniform across all cities. These differences may reflect the contrast between gridded reanalysis and station-based satellite-derived estimates, local representativeness at individual sites, and differing treatment of cloud and atmospheric conditions. Overall, the comparison indicates that dataset choice can affect variability estimates at specific locations, and further analysis using gridded satellite-derived data would help quantify differences in seasonal and annual variability between reanalysis and satellite-based products.

4. Conclusion

This study addresses a critical knowledge gap by quantifying interannual irradiance variability across Canada's full geospatial extent, including underserved regions above 58°N. Analysis of interannual COV over a 25-year period from 1998-2022 using ERA5 reanalysis data demonstrated substantial regional differences in annual solar resource variability, particularly in Northern Canada and coastal regions.

The results show that annual GHI is relatively stable, with COV <5% in most regions, while BHI exhibits substantially higher variability (between 5-18% COV in most regions) because of its stronger dependence on atmospheric conditions. Monthly COV analysis further demonstrates that seasonal variability can exceed annual variability and should be considered when assessing PV performance, project bankability, storage needs, and grid reliability. The comparison with CWEEDS indicates that reanalysis and satellite-derived datasets may produce broadly similar ranges of COV but will differ depending on location. Robust solar resource assessment therefore depends on both the temporal scale of analysis and the characteristics of the underlying weather dataset. These findings support PV system bankability, grid reliability assessment, and renewable energy planning in high-latitude environments.

5. References

Aron Habte., *et al*. 2020. Long-Term Spatial and temporal solar resource variability over America using the NSRDB version 3 (1998-2017). Volume 134, *Renewable and Sustainable Energy Reviews.* DOI: https://doi.org/10.1016/j.rser.2020.110285 (Accessed on 19-02-2026).

Gerald M. Lohmann *et al*. 2016. Local short term variability in solar irradiance. *Atmospheric Chemistry and Physics,* volume 16, issue 10. DOI: 10.5194/acp-2016-2 (Accessed on 19-02-2026).

Hersbach H, *et al*. 2023. ERA5 hourly data on single levels from 1940 to present. Copernicus Climate Change Service (C3S) Climate Data Store (CDS), DOI: 10.24381/cds.adbb2d47 (Accessed on 19-02-2026).

Natural Resources Canada. 2022. Canadian Weather Energy and Engineering Datasets (CWEEDS). *Open Government*. https://open.canada.ca/data/en/dataset/005494f2-1848-48d5-abe4-a76a7846f035 (Accessed on 13-03-2026).

Robert J. Davy, Alberto Troccoli. 2012. Interannual variability of solar energy generation in Australia. *Solar Energy*, Volume 86, Issue 12, pg 3554-3560. DOI: 10.1016/j.solener.2011.12.004. (Accessed on 19-02-2026)

Sami K. Solanki, Natalie A. Krivova, Joanna D. Haigh. 2013. Solar Irradiance Variability and Climate. *Annual Review Astronomy and Astrophysics*. 51:311-351. DOI: 10.1146/annurev-astro-082812-141007 (Accessed on 19-02-2026).

Tonita, E. M., Bardy, D. A., Richardson, G., Weir, K. R., and Mesquita, L. Benchmarking satellite & reanalysis irradiance products in Canada: A multi-model validation using research-grade and non-reference ground networks. *Under review for publication July 2026*.

Yang, D., and Bright, J. M. Worldwide validation of 8 satellite-derived and reanalysis solar radiation products: A preliminary evaluation and overall metrics for hourly data over 27 years. *Solar Energy*, volume 210. DOI: https://doi.org/10.1016/j.solener.2020.04.016 (Accessed on 19-08-2026).